Research Article

Stability Analysis of the Shiliushubao Landslide Based on Deformation Characteristics and External Trigger Factors in the Three Gorges Reservoir

Guilin Luo [1,2] **Guangming Ren,**[1] **Xiaojun Bao,**[2] **Xili Yang,**[1] **and Teng Liu**[1]

[1]*State Key Laboratory of Geo-Hazard Prevention and Geoenvironment Protection, Chengdu University of Technology, No. 1 Erxianqiao East Road, Chengdu 610059, China*
[2]*School of Civil Engineering and Mechanics, Lanzhou University, Lanzhou 73000, China*

Correspondence should be addressed to Guilin Luo; luogl15@lzu.edu.cn

There exists the problem of landslide reactivation due to the seasonal fluctuation of rainfall and reservoir water level annually. Based on a large number of GPS monitoring data of the landslide mass after impoundment of the Three Gorges Reservoir in Shiliushubao landslide area, the relationship between the external trigger factors and slope stability could be obtained. A finite element calculation model has been established for the stability analysis of the Shiliushubao landslide after impoundment from January 2004 to October 2009. Through the deformation characteristics of the landslide, it is shown that the landslide exhibited a stepwise pattern on the whole, which developed faster after impoundment and slowed down in rainy seasons. The trend of the curve kept roughly opposite to the fluctuation of the safety factor. It suggested that the stability of the landslide mass was closely related to the seasonal fluctuation of the rainfall and the reservoir level, and the landslide deposits demonstrated to be reactive with them. The subject provides a certain reference value on the landslide stability analysis and the risk assessment within a similar engineering geological condition.

1. Introduction

Landslide and floods in China are a large amount of socioeconomic disruptions, property damages, and casualties, and they are caused by multiple factors including the geography [1, 2], the geological tectonism [3–5], hydraulic alteration [6], flood alluvial [7], earthquake [8, 9], climate change [10, 11], and anthropogenic engineering constructions [12]. The Three Gorges Dam has provided huge hydropower resources and mitigated the devastating effects of deluges with time tested for the past decades ago [13, 14], while there exists some geological disasters owing to the drastic fluctuation of the reservoir water level.

In the recent years, the researchers have found that the changes of the water level would affect the safety of the reservoir bank via numerical simulation [15, 16] and/or field investigation [17, 18]. The hydraulic conductivity and the rate of the water level changes dominate the transient flow response which directly controls the stability of the landslide [19, 20]. The pore pressures and the water surface pressure can also affect the stability of the landslide [21, 22] in the form of drag force outside the slope and impair the soil shear strength and the geophysical characteristics [23, 24]. Furthermore, the study of the rainfall diffusion in the soil also reveals the mechanisms of the landslide to eventually result in slope failure [25, 26].

All experimental works have their limitations, either due to the difficulties or ambiguity in filed investigations or measuring some quantities [27, 28], mainly due to the complexity of the test process. Numerical simulations and field investigations are widely used to study the deformation and the stability mechanism of the landslide [29], and there are a few research studies attending to apply the integrated

monitoring system to a single landslide and combine the numerical model results [30, 31].

In the present study, a generalized model was selected to represent the landslide on the north bank of the Yangtze River, and the nonlinear seepage field of the bank was considered to realize the real-time changes. Combined with the field investigation data, the numerical analysis using Comsol Multiphysics was conducted to investigate the dynamic failure process of the landslide mass under the fluctuation of the reservoir water level and precipitations. In the whole process, this subject attended on the evolution of the changes of the safety factors to determine the changes of the stability of the reservoir bank with the grey relational grade. The results of the numerical modeling and the surface deformation were able to accurately explain why the stability of the Shiliushubao landslide increased as the reservoir water level rose, whereas it decreased as the reservoir water level dropped during the flood season.

2. Description of the Shiliushubao Landslide

The Shiliushubao landslide is a part of the Huanglashi landslide, situated in 1.5 km downstream of Badong Country and 66 km upstream of the Three Gorges Dam. Along the north bank of the Yangtze River, the planar shape of the landslide mass approximates a square of length 500–550 m and a width of 350–470 m. The average thickness of the sliding mass has an average of about 40–50 m, and an area of $25.2 \times 10^4 \, m^2$ with an estimated volume of $12 \times 10^6 \, m^3$. The sliding direction is 25°N, which is approximately perpendicular to the Yangtze River. The vertical height of the landslide is about 320 m, and its elevation ranges from 40 to 320 m, with an average slope angle of about 28°. The right and left sides are bounded by the gully, and the trailing edge is bounded by a group of steep walls. In addition, the field survey indicated that two secondary shallow sliding blocks have developed near the river (Figure 1).

There are totally fifteen GPS stations on the landslide mass monitoring the surface deformation, and these station distributions are all shown in Figure 2. In order to monitor the deformation of the whole area, the GPS stations were roughly uniformly placed near the three survey lines. These three survey lines were established for borehole distributions which could directly and accurately identify stratigraphic. Different from other projects, five GPS stations were placed at the leading edge, which may be more comprehensive to reflect the fluctuations of the landslide stability. Besides, there exists three points for the reservoir water level and rainfall in the upper part of the landslide.

The geological units and structures of the landslide mass were analyzed on the early materials which were obtained from field investigations and explorations. The engineering geological profile proved that the sliding deformation occurred along the contact surface between the deposits and the bedrock (Figure 2). The landslide mass consists of the full weathering or strong weathering red broken calculates with some clastic rock, and the bedrock mainly consists of grey, thin to medium-thick layer of interbedded dolomitic limestone and partially the purple-red mudstone of Badong

Formation from the Triassic. From the formal lecture, the stratum of the Badong Formation was always called the "easiest sliding strata" in China due to its special geophysical characteristics and low strength. The geophysical characteristics and hydraulic properties are given in Table 1.

As the erosion of the strong weathering deposits, long-term water softening, and rainfall infiltration, there are numerous cracks and subsidence features observed at the slippery tongue and the trailing edge of landslide of the landslide body, especially those in the rear part are turned out to form a continuous crack within the landslide deposit. From the field explorations, the largest crack was around 344 m long with an opening width of 1–45 cm, a roughly depth of 10–110 cm, and a dip-slip dislocation of 2–150 cm until 2009. The maximum accumulated surface deformation from January 2004 to December 2009 reached 1485 mm. These cracks and apertures proved good tunnels for seepages and may cause extra pore pressures to the slides.

The special topography, lithology, and geological structure of the landslide area are the pivotal factors of landslide formation and control the deformation and evolution of the prestable landslide. In addition, the project finally compared the deformation and the landslide stability results and summarized the dominant factors which drove landslide reactivation, i.e., the seasonal fluctuation of rainfall and reservoir level of the Three Gorges Reservoir. The water level change will induce the growth of landslide mass, and the rainfall will accelerate the deformation of the landslide mass. The seasonal fluctuations of the water level during the operation of the reservoir and the increase of the rainfall capacity dramatically change the hydrogeological conditions of the landslide mass and reduce the strength of the soil.

3. Monitoring Data and Analysis of Deformation Characteristics

3.1. Monitoring Data. In early years, the slope was confirmed to undergo noticeable deformation and cracks, and this information was reported to government by local people. Therefore, the special monitor area was established for deformation and rainfall of the landslide slope. The accumulated displacement and water level fluctuation versus time curve is plotted in Figure 3 along with the surface deformation, reservoir water level, and rainfall capacity monitoring data since January 2004 to October 2009.

As seen from the curves of the reservoir water level, the reservoir water level remained approximately constant over 135 m, and its variation tendency is essentially synchronous to the rainfall capacity. In the large rainfall months, especially rainy seasons, the water level is always on the rise, and the highest water level was 169.7 m in December 2006. With the period of low precipitations, the reservoir water level fluctuation is in base volatility, and the water level changes are in the range of 1-2 m. In 2007–2009, the rainfall was much larger than the other years, and the water level fluctuations were at around 12–20 m. Based on the data comparison of the average velocity of the impoundment and drawdown of per month, the trend of water level changing can be observed by their difference to some extent (Figure 4).
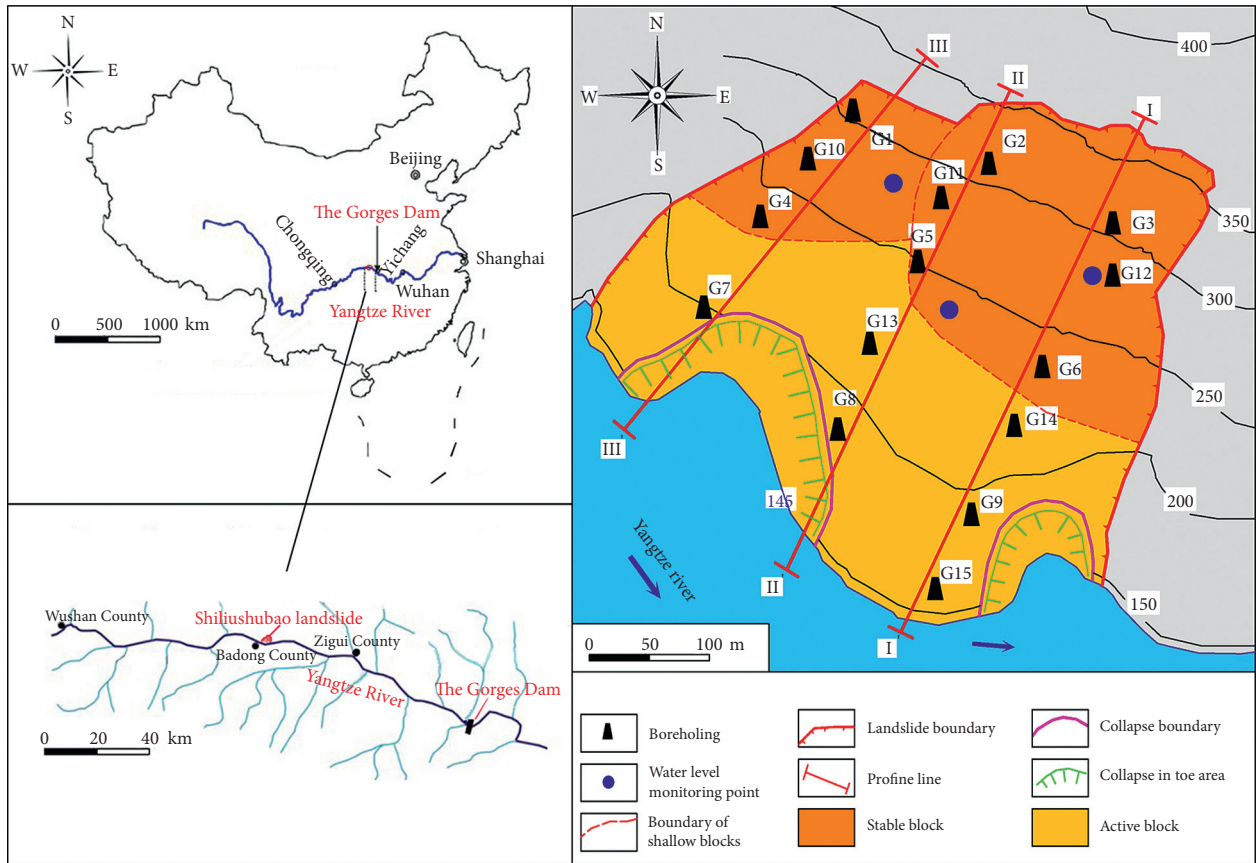
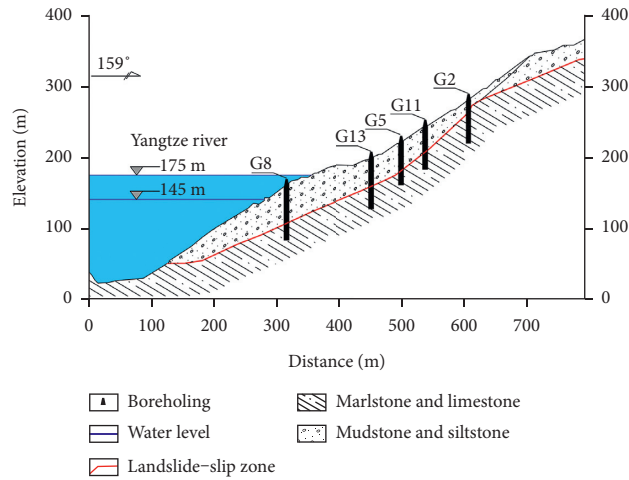FIGURE 1: Location distribution and geological map of the Shiliushubao landslide.

FIGURE 2: Geological map of the section II-II' of the landslide.

TABLE 1: Geophysical characteristics and hydraulic properties of the study area.

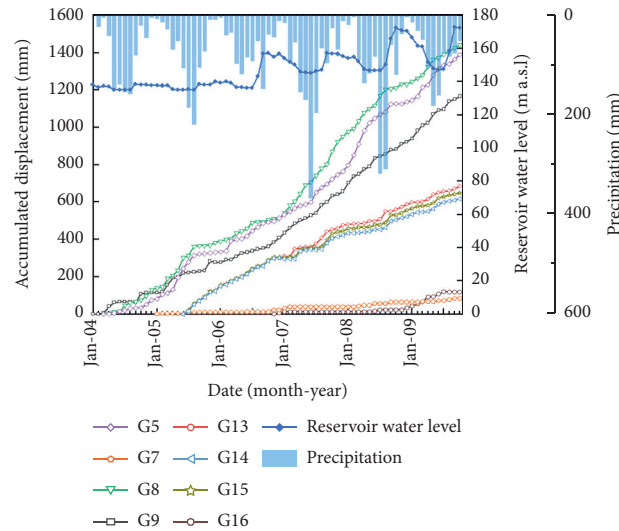| Rock category	ρ (g/cm^3)	E (GPa)	μ	φ (°)	c (MPa)	K (×10^{-4} m/s)
Landslide deposit	2.61	0.45	0.27	38	0.15	0.067
Bedrock	2.75	12.5	0.25	45	0.8	0.048

Figure 3: Accumulated displacement of GPS stations, reservoir water level, and precipitations from January 2004 to October 2009.

It roughly reveals that the landslide mass exhibited a stepwise deformation characteristic, especially occurred on the active blocks since the implementation of the professional monitoring in 2004 which can be reflected by the accumulated displacement curve of the GPS station points of the landslide mass (Figure 4(a)). The total displacement of G5, G7, and G8 was placed in front of the landslide maintain sustained growth from 2004 to 2009, which suggests that the slope was marginally stable or unstable and maybe revival for complexity external trigger factors (Figure 5). In 2004, there are few GPS stations effected by these factors, and the average daily deformation is lower than 4 mm/d that suggested that the middle and rear parts of the landslide remained stable. During 2007–2009, the reservoir water level changed substantially at the elevation of 145–169 m, and the accumulated deformation increased significantly.

It is clear that the accumulated surface displacement curves always increase sharply after drawdown in May–July every year and remain or increase relatively slowly after impoundment from September to April. Correlated to the collapses, precipitations, and reservoir water level fluctuations at the leading edge of the landslide, the accumulated surface displacement near these stations grows continually, in which the stepwise growth is not as clear as before from 2007 to 2008, showing prominently at the station of G7, G8, and G9. In the heterogeneity and anisotropic stratum, the groundwater level rise at a slower rate than the reservoir water level. There exist some progressive cracks in the landslide, such as the shear cracks at the leading edge and tension cracks at the trailing edge. Everytime the reservoir water level rises, the leading edge of the landslide may be submerged. The hydrostatic pressure increases on the landslide surface which directed inside the slope, and the overall landslide remains steady and the monthly deformation is relatively stable [32]. On its reverse side, the groundwater level would always lag behind the reservoir

water level, and the hydrodynamic pressure would directly act in the sliding section, directed outside the slope (Figure 6). Furthermore, the rainfall infiltration may weaken the mechanical properties of the rock mass that may also decrease the landslide stability.

3.2. Analysis of the Deformation Characteristics of the Landslide Mass.
According to the results shown in Figure 4, these deduced that the increase of the accumulated displacement was relatively large. Based on the field investigations, the internal deformation mainly rose parallel to the sliding direction. The closer to the collapse boundary, the larger the displacement is, while the increase of the displacement of the other station points is relatively small [33–35].

It is reflected in Figure 4 that the annual displacement of G5, G8, G9, and G13 is much larger than other GPS station points, in which the average displacement rate of these fluctuated between 0.89 and 3.65 mm/d, and the rate of GPS-3 and GPS-6 fluctuated between 0.55 and 1.68 mm/d. The other station points were under 0.55 mm/d or nearly unchanged.

Combining Figure 5, it could be seen that the fluctuation of the reservoir water level in 2004, 2005, and 2006 were stable, and the rate of the annual displacement changed significantly after drawdown. Especially in 2006, the rainfall was little higher than 2004 and 2005, and the increase of the displacement of the landslide was smaller. However, in 2007, the displacement of the landslide changed not as that in 2004–2006, while the rainfall was much bigger than the past three years in the flood season, in which the highest precipitation reached to 367.9 mm in June 2007. Too much rainfall caused the rate of the annual displacement of the landslide increased; but unlike the formal, the accumulated displacement in 2007 grew consistently, in which the maximum displacement rate of the
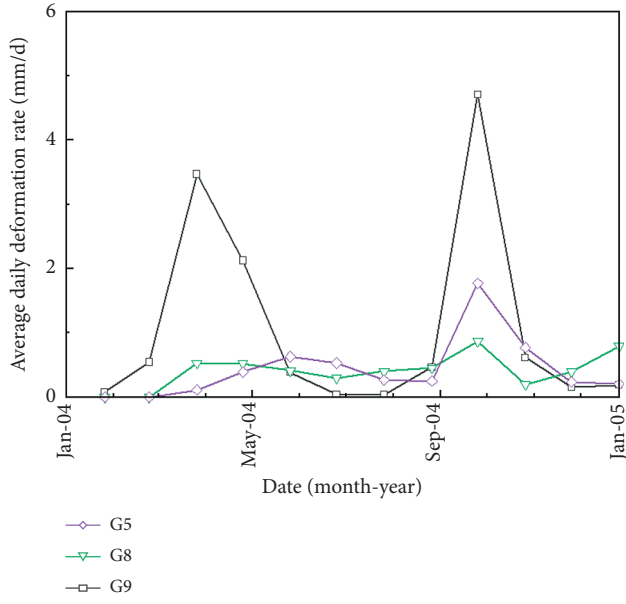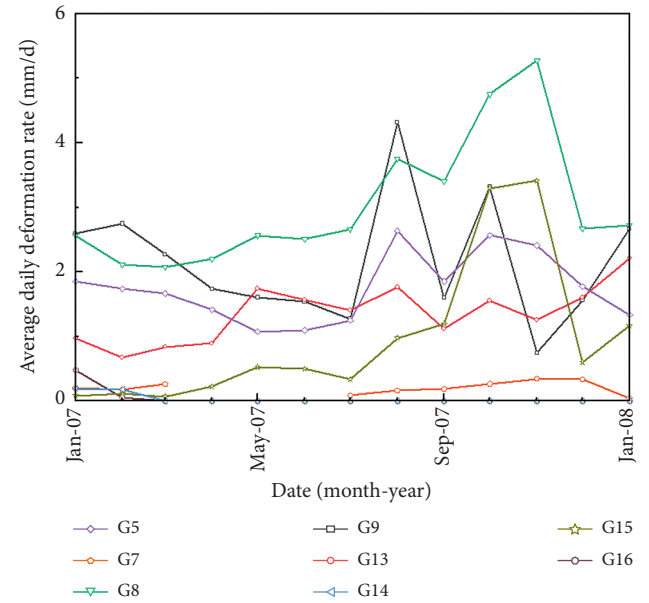
(a)
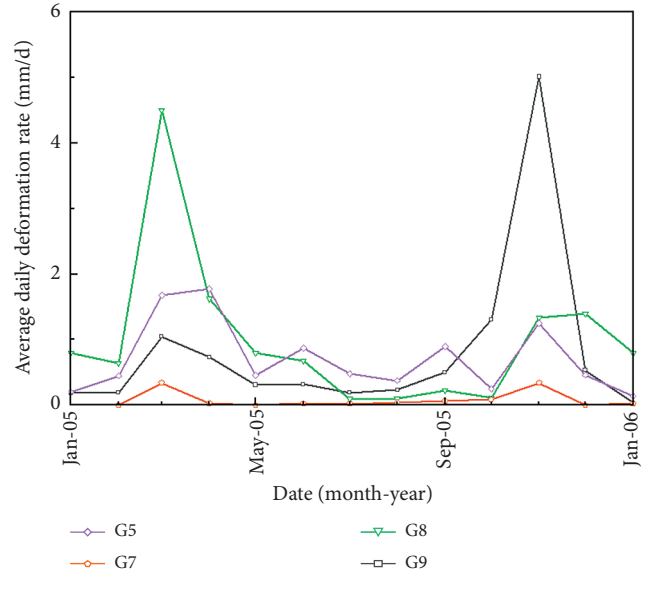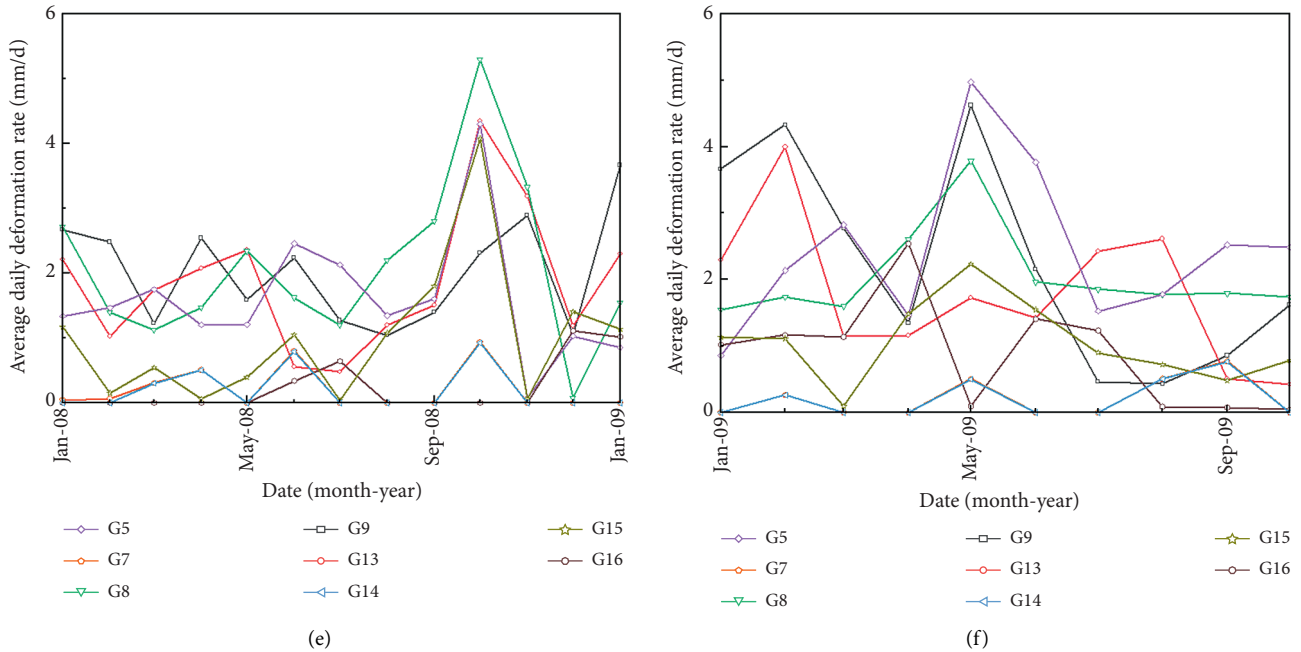
(b)
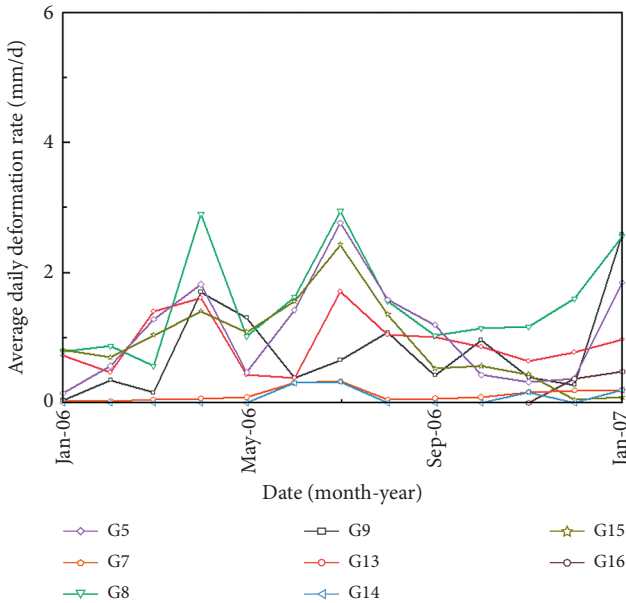
(c)

(d)

Figure 4: Continued.

(e)

(f)

FIGURE 4: Curves of daily mean displacement rate of each month from January 2004 to September 2009. (a) From January 2004 to January 2005; (b) from January 2005 to January 2006; (c) from January 2006 to January 2007; (d) from January 2007 to January 2008; (e) from January 2008 to January 2009; (f) from January 2009 to October 2009.
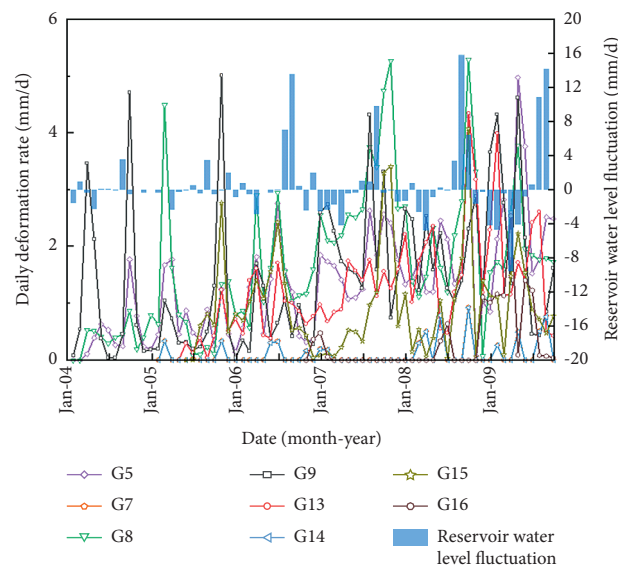

FIGURE 5: Accumulated daily deformation rate of GPS stations and reservoir water level fluctuation from January 2004 to October 2009.

monitoring points reached 4.46 and 5.31 mm/d. Therefore, the rate of the annual displacement of these stations to the collapse boundary increased substantially. There were two months in which the precipitation was over 300 mm in 2008, and the displacement rate decreased relatively after impoundment, with rapid increase after drawdown. Everytime the reservoir water level is rising high, the rate of the deformation would increase significantly after the reservoir water level dropped, and the accumulated displacement would become steps in several months. As the

reservoir water level rose too high in 2008, there were several months for reservoir water dropping at the beginning of 2009, and the displacement rate of these monitoring stations was kept elevated.

Based on the monitoring materials, the sliding process only progressed to the mediocre part; the back part of the landslide mass was merely slightly deformed. Following this trend, if the landslide was not reinforced, the rear part would have to fail when the sliding of the average part supplied sufficient space to move.
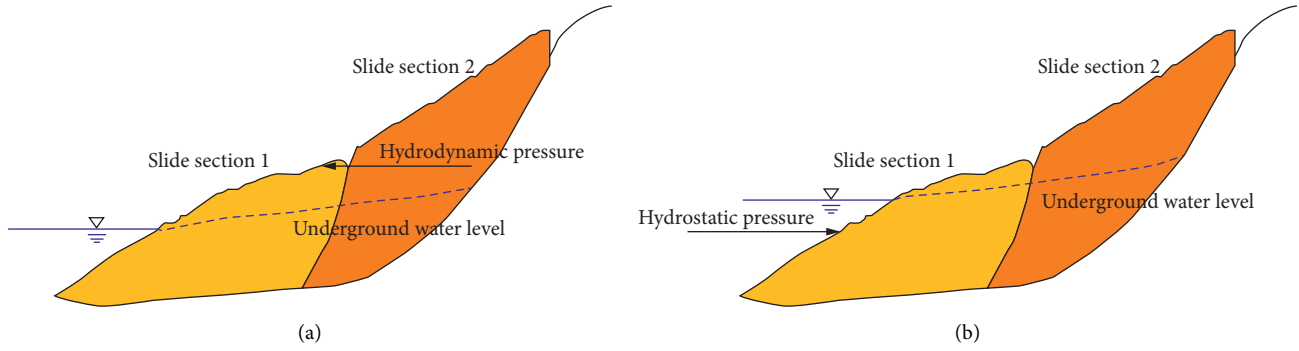
FIGURE 6: The schematic diagram of hydraulic action acting on the slide of Shiliushubao landslide.

4. Stability Analysis of Water Level Fluctuation

4.1. Numerical Modeling and Calculation Conditions. uA numerical calculation model of the slope had been established based on the geological engineering section II-II$'$ (denoted in Figure 7). The boundary of the model could be given as this: the bottom periphery elevation of the model is approximately 0 m, the height of the right periphery is around 368 m, the left periphery is around 42 m, and the horizontal distance is around 794 m. There has been set two kinds of materials in the model, the bedrock and the landslide body, which are all assumed as elastoplastic material that the yield conditions satisfied the Mohr–Coulomb criterion [36].

When simulating the two-dimensional finite element seepage in the Multiphysics, the progress of the subsurface flow first adopts the two-phase Darcy's law model and then combines the soil mechanics [37]. The transient seepage analysis is conducted based on the actual reservoir water level (Figure 3) parallel to the monthly precipitation (equation (1)) [38]. Then, the pore pressure calculations join up the stability analysis with the shear strength reduction, which is realized by reducing the variables c and φ while defining the parameter SRF and accumulating the results till the critical state (equation (2). Also, there are two parameters to define the saturated area and unsaturated area with its built-in function Hp, which defines the pore pressure in the soil.

$$
\begin{cases}
\dfrac{\partial}{\partial x}\left[K_x \dfrac{\partial H}{\partial x}\right] + \dfrac{\partial}{\partial y}\left[K_y \dfrac{\partial H}{\partial y}\right] + \dfrac{\partial}{\partial z}\left[K_z \dfrac{\partial H}{\partial z}\right] + W = S_s \dfrac{\partial H}{\partial t}, \\[2mm]
H(x,y,z,t)|_{t=0} = H_0(x,y,z), \quad (x,y,z) \in \Omega, \\[2mm]
K \dfrac{\partial H}{\partial n}\bigg|_{\Gamma_2} = q(x,y,z,t), \quad (x,y,z) \in \Gamma_2,
\end{cases}
\tag{1}
$$

where K_x, K_y, and K_z are the values of hydraulic conductivity along the x, y, and z coordinate axes, which are assumed to be parallel to the major axes of hydraulic conductivity; H is the potentiometric head; W is a volumetric flux per unit volume representing sources and/or sinks of water; S_s is the specific storage of the porous material; t is the time; q is the flux.

$$
\begin{cases}
c' = \dfrac{c}{\mathrm{SRF}}, \\[3mm]
\tan \phi' = \dfrac{\tan \phi}{\mathrm{SRF}}.
\end{cases}
\tag{2}
$$

During the numerical computing process, c is the cohesion; φ is the internal friction angle; and Fr is the factor of safety. The trail of Fr incrementally increases until the convergent criterion is not satisfied.

For boundary conditions, the interface, i.e., the sliding surface of this landslide, which is between the landslide mass and the bedrock, is taken as impermeable, for it is nearly three orders of magnitudes of hydraulic conductivity larger than other materials. To fit the reality, there establishes a subordinate landslide-slip zone. The saturated hydraulic conductivity k_s of the landslide mass in the Gorges Reservoir region could vary from 1×10^{-4} m/s to 1×10^{-7} m/s, and this subject finally uses those given in Table 1 combining with the velocity of impoundment and drawdown. The other physical and mechanism parameters are all obtained from early in situ tests and laboratory experiments, such as the packer permeability test, specific gravity test, and consolidated drained triaxial compression test.

4.2. Numerical Simulation Results for Stability. Figure 8 illustrates the results of the variations of the safety factor from January 2004 to October 2009, as obtained from the fluid-soiled coupling analysis. From Figure 8, the fluctuation of the landslide stability could be approximately divided into two parts with the factor of safety. One part is from January 2004 to October 2006, the fluctuation is slight, and it keeps relatively high. The other is from November 2006 to October 2009, the fluctuation decreases sharply, and it keeps relatively low. The increase of the external trigger factors may cause disequilibrium and large deformation in the slope.

The precipitations during January 2004 to July 2006 were around 42–80 mm/month; thus, the reservoir water level was maintained at 135–138 m. And the factor of safety was between 1.12 and 1.2, which demonstrates that there was no trend to slide in the landslide mass, and the slope is primarily
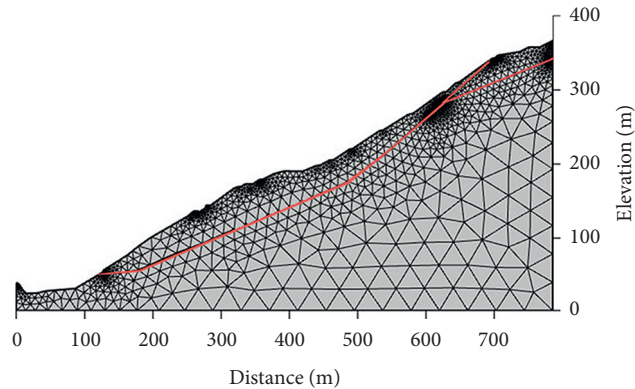
FIGURE 7: Numerical model of the section II-II′ for slope stability analysis.
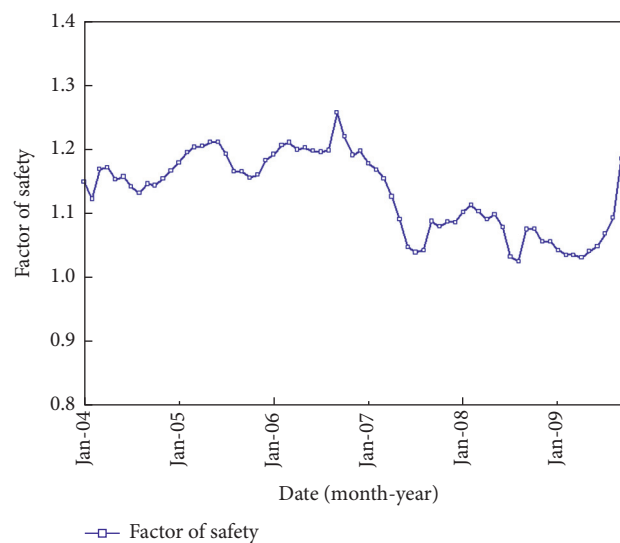

FIGURE 8: Factor of safety of section II-II′ from January 2004 to October 2009.

kept stable. While the precipitations grew obviously in rainy seasons in 2006, the factor of safety grew parallel to the reservoir water level from 1.17 to 1.26. On the contrast, the factor of safety fluctuated sharply after impoundment until the next rainy season and reached the minimum of 1.04. The accumulated displacement grew constantly in the whole process, and there existed an acceleration phase in 2006 after impoundment (Figure 3). It suggests that there was some insurance that the landslide might become disequilibrium. After the lower peak of this curve, the factor of safety grew corresponded to the rainy season in 2007, conforming to the general change of fluctuations of the factor of safety. While the increase of the factor of safety was not as much as the formal one in 2006, the reservoir water level kept high between 147 and 172 m, which just kept from 1.04 to 1.15. The accumulated displacement assumed stepwise growth more obviously, and the rate of displacement was higher and more periodical. Generally speaking, the rate of surface landslide deformation decreased as the reservoir water level rose after the reservoir impoundment, whereas it increased with the water level fell.

4.3. Sensitivity Analysis for Stability.

The curve of the safety factor is approximately synchronous with the water level change, but always lags behind compared with the reservoir water level. The water level fluctuations may assist to predict the stability of the slope which is mainly driven by the seepage field in a sense (Figure 9), but it could not directly represent the variation of stability which requests actual external trigger factors.

Figure 9 shows the relationship between the rate of factors of safety with the velocity of water level change, which represented the different stages the landslide mass might have experienced. The reservoir water level fluctuations could be approximately divided into four types throughout the calculation process with its velocity. Same as the variation of the water level, these curves could not directly respect the relationship between the factor of safety with the reservoir water level. Since the impoundment of the reservoir, the leading edge of the landslide may be submerged by the water level that would increase the hydrostatic pressure, which is conducive to the landslide stability. In the process of the reservoir impoundment, the faster the velocity
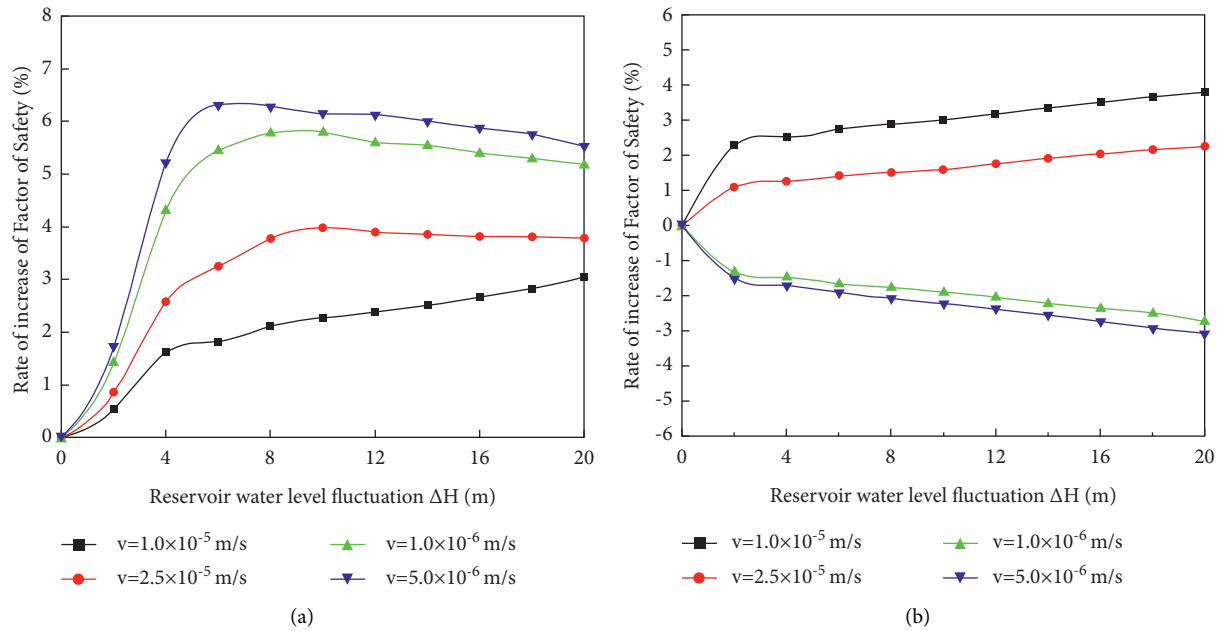
FIGURE 9: Sensitivity analysis of slope stability conditions. (a) Reservoir storage; (b) reservoir water level drawdown.

is, the faster the safety factor would increase. However, if the velocity is too much bigger than the hydraulic conductivity, the increase rate would gradually slow down as the water level rises. The closer the values are, the greater the height of the water level where the incremental slowdown occurs. It suggests that the impoundment would improve the stability of the landslide mass [39, 40].

The drawdown of the reservoir water level may cause the hydrodynamic pressure in the rear edge of crack particularly prominent. On the contrast, it shows two different types in the process of drawdown. As the hydraulic conductivity is closed to the velocity of the water level fluctuation, the factor of safety was not just decreased. When the velocity of the water level fluctuation is less than the hydraulic conductivity, the safety factor increases and the rate is small. However, these kinds of conditions would not actually occur, and this analysis is only based on theoretical exploration. The further reason may be the lagging drainage of the groundwater, inducing the excretion of the water in the landslide mass lags behind the reservoir water. It suggests that the drawdown would reduce the stability of the landslide mass at some extent.

5. Discussion

After the analysis of the landslide deformation characteristics and numerical model calculating, the seasonal fluctuation of rainfall and reservoir level plays significant roles in the landslide stability. The characteristics of the landslide deformation could guide the analysis of the stability, and it may be the tight data for the field research work [28, 41].

These figures have shown the relationships between the surface accumulated displacement, the stability of the landslide mass and the fluctuation of the reservoir water level, as all of them have an important correlation. The

surface accumulated displacement curves has a palpable stepwise increment in rainy seasons each year, and the safety factor keeps relatively similar. If the slope keeps marginally stable, the slightest changes of the external trigger factors may lead to disequilibrium and significant deformations [42]. Table 2 summarizes the input items for the factor of safety and the displacement of G5 station.

Based on the grey relation analysis, the grey relation grade (GRG) is useful to evaluate the degree of relationship between the input and extra factors. The GRG ranges from 0 to 1; according to the assumption of the method, a value of 0.6 or higher proves a strong relationship towards these. Table 2 provides the mainly factors influencing the safety factor and the landslide deformation. They both correspond to the rainfall and water level fluctuations and always lag behind the precipitations. When the water level rises, the accumulated surface displacement curve is relatively stable or grows slowly, and the landslide mass will keep steady or the stability might be limited increasing [43]. At this time, the water level of the Gorges region drops rapidly or runs at a low elevation, and the rate of the surface displacement changes significantly, with the stability of the landslide decreasing.

Upon combining the factor of safety with the surface displacement monitoring results obtained after the reservoir water level fluctuated (Figure 10), it is suggested that the numerical modeling results demonstrate why the deformation rate of the Shiliushubao landslide decreased as the reservoir water level increased, and the deformation rate was negatively correlated with the reservoir filling. The permeability limited the excretion and replenishment of water in the soil. Everytime there is the reservoir water level drawdown, it causes the seepage force and extra pore pressure to the landslide. And if the reservoir water level remains relatively constant after increased, the extra pore water pressure

TABLE 2: The grey relational grade (GRG) between the influencing factor with factor of safety and displacement.

| Input	Influencing factors	GRG
	Input 1, the 1-month cumulative antecedent rainfall	0.626
	Input 2, the 2-month cumulative antecedent rainfall	0.605
	Input 3, reservoir level change in the 1-month period	0.681
Factory of safety	Input 4, reservoir level change in the 2-month period	0.703
	Input 5, the average elevation of the reservoir level in the current month	0.610
	Input 6, the displacement of G8 over the past 1 month	0.604
	Input 7, the displacement of G5 over the past 1 month	0.608
	Input 8, the 1-month cumulative antecedent rainfall	0.664
	Input 9, the 2-month cumulative antecedent rainfall	0.662
The displacement of G5	Input 10, reservoir level change in the 1-month period	0.672
	Input 11, reservoir level change in the 2-month period	0.662
	Input 12, the average elevation of the reservoir level in the current month	0.761
	Input 13, the displacement of G8 over the past 1 month	0.941

(a)

(b)

(c)
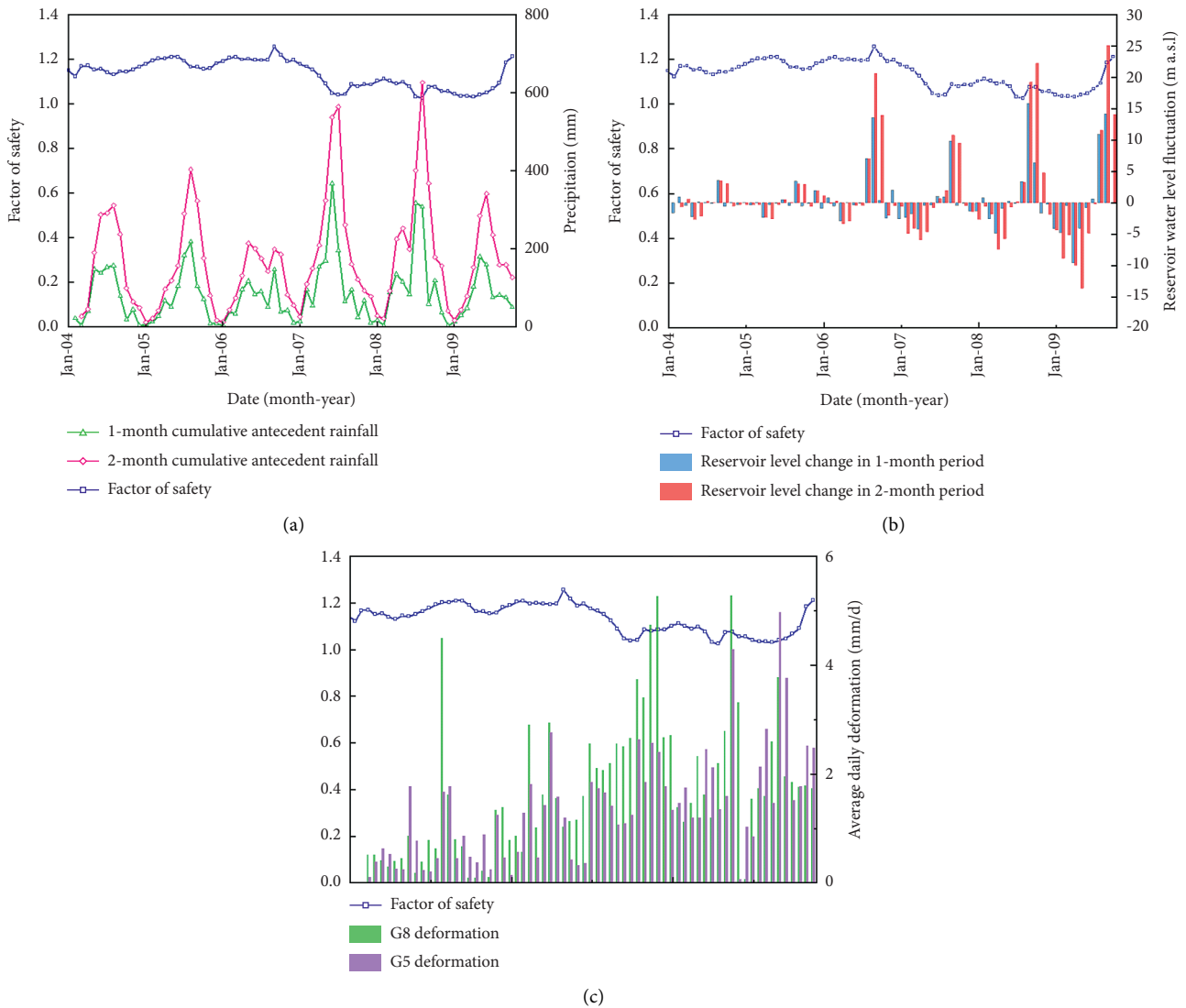
FIGURE 10: External trigger factor analysis with the factor of safety. (a) Accumulated antecedent rainfall; (b) reservoir water level fluctuation; (c) average daily deformation.

would dissipate progressively, which may improve the stability of the landslide and the rate of the deformation would imperceptibly keep steady [44]. From accumulated displacement curves, there exists a stepwise character. Compared with numerical simulation, a simple deformation feature analysis has lower accuracy in determining slope stability.

After calculating the transient safety factor of the slope with multiple rainfall combinations, it is suggested that with the infiltration of the rainwater and its movement within the slope body, the safety factor changes, indicating that in addition to the time effect, there is also a spatial effect. While it is difficult to assess the stability of the landslide mass with numerical simulation on a scene, the external performance becomes necessary then. And the behavior of slopes subjected to water level fluctuations and landslide deformation are increasingly the subject of scientific attention and research.

6. Conclusion

The Shiliushubao landslide is an emblematic slope failure in Huanglashi landslide which is influenced evidently by the water level in Three Gorges Reservoir region. Based on investigation and simulation analyses, these following conclusions were made.

(1) According to the analysis of GPS surface deformation monitoring of the landslide, the displacements obtained by these GPS stations on the active blocks were relatively large and escalated with time, while the increase of the displacements on the other stations was approximately small in the whole monitoring process. With this trend, if the landslide is not reinforced, the rear part would fail when the sliding of the middle part supplies sufficient space to move.

(2) The calculation results for landslide stability show that the reactivation triggering factors are mainly corresponded to the water level variations and precipitations. While the process of the reservoir drawdown, the decrease of the groundwater level of landslide lags behind the reservoir water level, which is a typical deterioration of the slope conditions, and increases the accumulated deformation. It shows that the stability is sensitive to the velocity of water level fluctuation.

Discussing the deformation and stability of the landslide, we quantify the importance of each factor on landslide occurrences, and we find that the drawdown of the water level of the Three Gorges Reservoir region could be summarized as the main controlling factor of the deformation of the landslide mass.

Data Availability

The data used to support the findings of this study are included within the article.

Disclosure

Chengdu University of Technology has bought the right for use of Comsol Multiphysics.

Conflicts of Interest

The authors declare that they have no conflicts of interest.

Acknowledgments

References

[1] M. S. Kim, Y. Onda, J. K. Kim, and S. W. Kim, "Effect of topography and soil parameterisation representing soil thicknesses on shallow landslide modelling," *Quaternary International*, vol. 384, pp. 91–106, 2015.

[2] L. Liucci, L. Melelli, C. Suteanu, and F. Ponziani, "The role of topography in the scaling distribution of landslide areas: a cellular automata modeling approach," *Geomorphology*, vol. 290, pp. 236–249, 2017.

[3] A. Agostini, V. Tofani, T. Nolesini et al., "A new appraisal of the ancona landslide based on geotechnical investigations and stability modelling," *The Quarterly Journal of Engineering Geology and Hydrogeology*, vol. 47, pp. 29–43, 2014.

[4] C. Mark, "An updated empirical model for ground control in u.S. Multiseam coal mines," *International Journal of Mining Science and Technology*, vol. 31, pp. 163–174, 2021.

[5] H. Rafezi and F. Hassani, "Drilling signals analysis for tricone bit condition monitoring," *International Journal of Mining Science and Technology*, vol. 31, pp. 187–195, 2021.

[6] J. M. Chang, H. Chen, B. J. D. Jou, N. C. Tsou, and G. W. Lin, "Characteristics of rainfall intensity, duration, and kinetic energy for landslide triggering in taiwan," *Engineering Geology*, vol. 231, pp. 81–87, 2017.

[7] S. Segoni, A. Rosi, D. Lagomarsino, R. Fanti, and N. Casagli, "Brief communication: using averaged soil moisture estimates to improve the performances of a regional-scale landslide early warning system," *Natural Hazards and Earth System Sciences*, vol. 18, pp. 807–812, 2018.

[8] K. Roback, M. K. Clark, A. J. West et al., "The size, distribution, and mobility of landslides caused by the 2015 m(w)7.8 gorkha earthquake, Nepal," *Geomorphology*, vol. 301, pp. 121–138, 2018.

[9] T. Wang, S. R. Wu, J. S. Shi, P. Xin, and L. Z. Wu, "Assessment of the effects of historical strong earthquakes on large-scale landslide groupings in the wei river midstream," *Engineering Geology*, vol. 235, pp. 11–19, 2018.

[10] M. Alvioli, M. Melillo, F. Guzzetti et al., "Implications of climate change on landslide hazard in central Italy," *The Science of the Total Environment*, vol. 630, pp. 1528–1543, 2018.

[11] D. J. Peres and A. Cancelliere, "Modeling impacts of climate change on return period of landslide triggering," *Journal of Hydrology*, vol. 567, pp. 420–434, 2018.

[12] S. Mohammadi and H. Taiebat, "Finite element simulation of an excavation-triggered landslide using large deformation theory," *Engineering Geology*, vol. 205, pp. 62–72, 2016.

[13] X. Q. Luo, F. W. Wang, Z. H. Zhang, and A. L. Che, "Establishing a monitoring network for an impoundment-

induced landslide in three gorges reservoir area, China," *Landslides*, vol. 6, pp. 27–37, 2009.

[14] M. Wang and J. P. Qiao, "Reservoir-landslide hazard assessment based on gis: a case study in wanzhou section of the three gorges reservoir," *Journal of Mountain Science*, vol. 10, pp. 1085–1096, 2013.

[15] J. C. Cai, N. P. Ju, R. Q. Huang et al., "Mechanism of toppling and deformation in hard rock slope: a case of bank slope of hydropower station, qinghai province, China," *Journal of Mountain Science*, vol. 16, pp. 924–934, 2019.

[16] X. R. Wang, Q. G. Rong, S. L. Sun, and H. Wang, "Stability analysis of slope in strain-softening soils using local arc-length solution scheme," *Journal of Mountain Science*, vol. 14, pp. 175–187, 2017.

[17] S. Alemdag, A. Akgun, A. Kaya, and C. Gokceoglu, "A large and rapid planar failure: causes, mechanism, and consequences (mordut, gumushane, Turkey)," *Arabian Journal of Geoscience*, vol. 7, pp. 1205–1221, 2014.

[18] J. Zhuang, J. Peng, G. Wang, I. Javed, Y. Wang, and W. Li, "Distribution and characteristics of landslide in loess plateau: a case study in shaanxi province," *Engineering Geology*, vol. 236, pp. 89–96, 2018.

[19] H. Hong, W. Chen, C. Xu, A. M. Youssef, B. Pradhan, and B. T. Dieu, "Rainfall-induced landslide susceptibility assessment at the chongren area (China) using frequency ratio, certainty factor, and index of entropy," *Geocarto International*, vol. 32, pp. 139–154, 2017.

[20] Z. L. Wei, Y. Q. Shang, H. Y. Sun, H. D. Xu, and D. F. Wang, "The effectiveness of a drainage tunnel in increasing the rainfall threshold of a deep-seated landslide," *Landslides*, vol. 16, pp. 1731–1744, 2019.

[21] A. A. E. Zehairy, M. M. Nezhad, V. N. Joekar, I. Guymer, N. Kourra, and M. A. Williams, "Pore-network modelling of non-Darcy flow through heterogeneous porous media," *Advances in Water Resources*, vol. 131, 2019.

[22] G. H. Wang and K. Sassa, "Pore-pressure generation and movement of rainfall-induced landslides: effects of grain size and fine-particle content," *Engineering Geology*, vol. 69, pp. 109–125, 2003.

[23] S. Matsuura, S. Asano, and T. Okamoto, "Relationship between rain and/or meltwater, pore-water pressure and displacement of a reactivated landslide," *Engineering Geology*, vol. 101, pp. 49–59, 2008.

[24] J. Zhao, J. Chen, X. Zhan, J. Ning, and Y. Zhang, "Distribution characteristics of floor pore water pressure based on similarity simulation experiments," *Bulletin of Engineering Geology and the Environment*, vol. 79, 2020.

[25] E. Conte and A. Troncone, "A performance-based method for the design of drainage trenches used to stabilize slopes," *Engineering Geology*, vol. 239, pp. 158–166, 2018.

[26] Y. G. Zhang, J. Qiu, Y. Zhang, and Y. Wei, "The adoption of elm to the prediction of soil liquefaction based on cpt," *Natural Hazards*, vol. 107, pp. 539–549, 2021.

[27] S. Shao, "A novel coating technology for fast sealing of air leakage in underground coal mines," *International Journal of Mining Science and Technology*, vol. 31, 2021.

[28] Y. Zhang, Z. Zhang, S. Xue, R. Wang, and M. Xiao, "Stability analysis of a typical landslide mass in the three gorges reservoir under varying reservoir water levels," *Environmental Earth Science*, vol. 79, 2020.

[29] L. K. Chen, L. Z. Jiang, H. X. Qin et al., "Nonlinear seismic assessment of isolated high-speed railway bridge subjected to near-fault earthquake scenarios," *Structure and Infrastructure Engineering*, vol. 15, pp. 1529–1547, 2019.

[30] L. K. Chen, A. Kurtulus, Y. F. Dong, E. Taciroglu, and L. Z. Jiang, "Velocity pulse effects of near-fault earthquakes on a high-speed railway vehicle-ballastless track-benchmark bridge system," *Vehicle System Dynamics*, vol. 25, 2021.

[31] L. K. Chen, P. Liu, L. M. Zhu, J. B. Ding, Y. L. Feng, and F. Moreu, "A simplified iterative approach for testing the pulse derailment of light rail vehicles across a viaduct to near-fault earthquake scenarios," *Proceedings of the Institution of Mechanical Engineers - Part F: Journal of Rail and Rapid Transit*, 2021.

[32] Y. G. Zhang, J. Tang, R. P. Liao et al., "Application of an enhanced bp neural network model with water cycle algorithm on landslide prediction," *Stochastic Environmental Research and Risk Assessment*, vol. 35, pp. 1273–1291, 2021.

[33] L. K. Chen, H. X. Qin, L. Z. Jiang, and L. Xu, "A vertical near-fault scenario earthquakes-based generic simulation framework for elastoplastic seismic analysis of light rail vehicle-viaduct system," *Vehicle System Dynamics*, vol. 59, pp. 949–973, 2021.

[34] W. Hou, H. Wang, L. Yuan, W. Wang, Y. Xue, and Z. Ma, "Experimental research into the effect of gas pressure, particle size and nozzle area on initial gas-release energy during gas desorption," *International Journal of Mining Science and Technology*, vol. 31, pp. 253–263, 2021.

[35] Y. Zhang, J. Qiu, Y. Zhang, and Y. Xie, "The adoption of a support vector machine optimized by gwo to the prediction of soil liquefaction," *Environ Earth Sci*, vol. 80, 2021.

[36] M. Xia, G. M. Ren, S. S. Zhu, and X. L. Ma, "Relationship between landslide stability and reservoir water level variation," *Bulletin of Engineering Geology and the Environment*, vol. 74, pp. 909–917, 2015.

[37] G. Wang, X. Qin, D. Han, and Z. Liu, "Study on seepage and deformation characteristics of coal microstructure by 3d reconstruction of ct images at high temperatures," *International Journal of Mining Science and Technology*, vol. 31, pp. 175–185, 2021.

[38] A. Corsini and M. Mulas, "Use of roc curves for early warning of landslide displacement rates in response to precipitation (piagneto landslide, northern apennines, Italy)," *Landslides*, vol. 14, pp. 1241–1252, 2017.

[39] Z. Dai, S. Chen, and J. Li, "Physical model test of seepage and deformation characteristics of shallow expansive soil slope," *Bulletin of Engineering Geology and the Environment*, vol. 79, 2020.

[40] Y. Zhang, Y. Xie, Y. Zhang, J. Qiu, and S. Wu, "The adoption of deep neural network (dnn) to the prediction of soil liquefaction based on shear wave velocity," *Bulletin of Engineering Geology and the Environment*, vol. 80, pp. 5053–5060, 2021.

[41] L. K. Chen, R. P. Yuan, X. J. Ji et al., "Modular composite building in urgent emergency engineering projects: a case study of accelerated design and construction of wuhan thunder god mountain/leishenshan hospital to covid-19 pandemic," *Automation in Construction*, vol. 124, 2021.

[42] B. Yang, K. Yin, S. Lacasse, and Z. Liu, "Time series analysis and long short-term memory neural network to predict landslide displacement," *Landslides*, vol. 16, pp. 677–694, 2019.

[43] Y. Zhang, S. Zhu, J. Tan, L. Li, and X. Yin, "The influence of water level fluctuation on the stability of landslide in the three gorges reservoir," *Arabian Journal of Geoscience*, vol. 13, 2020.

[44] Y. Zhang, S. Zhu, W. Zhang, and H. Liu, "Analysis of deformation characteristics and stability mechanisms of typical landslide mass based on the field monitoring in the three gorges reservoir, China," *Journal of Earth System Science*, vol. 128, 2018.